ANL/CP--70626

DE92 004143

ACTIVATION ANALYSES FOR DIFFERENT FUSION STRUCTURAL ALLOYS *

H. Attaya and D. Smith
Argonne National Laboratory
Argonne, IL 60439-4832
(708) 972-4484

The leading candidate structural materials, viz., the vanadium alloys, the nickel or the manganese stabilized austenitic steels, and the ferritic steels, are analysed in terms of their induced activation in the TPSS fusion power reactor. The TPSS reactor has 1950 MW fusion power and inboard and outboard average neutron wall loading of 3.75 and 5.35 MW/m^2respectively. The results shows that, after one year of continuous operation, the vanadium alloys have the least radioactivity at reactor shutdown. The maximum difference between the induced radioactivity in the vanadium alloys and in the other iron-based alloys occurs at about 10 years after reactor shutdown. At this time, the total reactor radioactivity, using the vanadium alloys, is about two orders of magnitude less than the total reactor radioactivity utilizing any other alloy. The difference is even larger in the first wall, the FW-vanadium activation is 3 orders of magnitude less than other alloys' FW activation.

* Work supported by the U.S. Department of Energy, Office of Fusion Energy, under Contract No. W-31-109-Eng-38.

Introduction

The materials neutron activation properties have increasingly acquired more influence on the materials selection for fusion reactors. In order to enhance the safety and the environmental attractiveness of these reactors, the induced radioactivities in these reactors should be minimized by the the appropriate choice of materials that have attractive short and long-term activation characteristics. It is essential, however, that materials used in fusion reactors must have high operational performance and long lifetime in the hard and the intense irradiation environment in these reactors. It is also important, in order for fusion reactors to compete economically with other energy resources, that the fusion reactor materials must be industrially and economically viable. The unit cost of a material and the cost of the associated research and development requirements are important factors. Yet, more crucial is the impact of the different material properties on the reactor operational performance and safety, the reactor lifetime, the cost of the safe disposal of the reactor waste during and after operation, and the potential of material recycling. All of these factors, appropriately weighted, should be considered in the selection process of fusion materials.

The Blanket Comparison and Selection Study (BCSS)[1], has evaluated the leading candidates structural alloys for the first wall/blanket of several design concepts of commercial fusion reactors. The materials considered are the austenitic steels, the ferritic steels, and the vanadium-base alloys. The results of this evaluation favor the vanadium alloys for the liquid lithium blanket concept. In this paper, we present activation analyses for the vanadium alloys and other leading structural alloys in the liquid lithium blanket of the Tokamak Power System Study (TPSS) reactor design [2]. Although calculations have been made for many variants of these alloys, we present here the analysis for only one representative alloy from each class of alloys. The PCA, the tenelon, the low activation HT9, and the V15Cr5Ti alloys are chosen to represent the nickel-stabilized austenitic alloys, the manganese-stabilized austenitic alloys, the ferritic alloys, and the vanadium-based alloys, respectively. The chemical compositions of these alloys are given in Table 1.

The TPSS reactor

The conceptual design of the TPSS reactor employs the self cooled lithium-vanadium concept, which is the top rated blanket concept in the BCSS. The TPSS design has 1950 MW fusion power, 6 m major radius, and 1 m minor radius. The neutron wall loading, as calculated by the NEWLIT code[3], varies from a maximum of 7.23 MW/m^2(at the outboard midplane) to a minimum of 3.48 MW/m^2(near the top of the inboard). The average neutron wall loading is 5.21 MW/m^2. The outboard and the inboard average neutron wall loadings are 5.35 and 3.75 MW/m^2, respectively.

Fig. 1 shows schematically the inboard and the outboard midplane radial build of the TPSS design. Natural lithium is used in the first wall (FW), the breeder, and the reflector. The structural material (SM), the V15Cr5Ti alloy, is used only in these zones. The FW is 1 cm thick and has equal volume fractions of Li and SM. The breeding zones are made of 92.5% Li and 7.5% SM. The inboard tungsten reflector (W_Ref) consists of 80% W (with .9 density factor), 10% Li, and 10% SM. The outboard Cao reflector (Cao_Ref) is composed of 80% Cao, 10% Li, and 10% SM. The steel shield (S_Sh) is made of 60% Fe1422 alloy, 30% TiH_2, and 10% He. The composition of the boron shield (B_Sh) is 60% B_4C, 30% Fe1422, and 10% He. It should be mentioned that the TPSS design has been optimized using the V15Cr5Ti alloy and in replacing this alloy with the other alloys, no attempts have been made to optimize the design for each alloy.

The transport calculations

Neutron transport calculations have been made, with the ONEDANT code[4], using the one-dimensional cylindrical toroidal geometry model. In this model, the cylinder axis is the vertical axis of the reactor and both the inboard and the outboard blankets/shields are modeled to take into account the geometrical toroidal effect as well as the mutual neutronics coupling between the inboard and the outboard blankets/shields. The transport calculation has been repeated for each alloy replacing the V15Cr5Ti alloy.

Fig. 1 shows also the neutron and photon fluxes for the V15Cr5Ti case (the TPSS reference design). For illustrative purpose, the 46 neutron groups fluxes produced by ONEDANT are collapsed into 5 major energy groups whose lower energies are 10 MeV, 1 MeV, 0.12 MeV, .87 eV, and 10-4 eV. Also, the 21 photon groups are collapsed into only one group. This figure shows clearly the effects of the different materials on the neutron flux. The large decreases of the low energy neutrons in breeder and in the FW zones, with their large natural Li contents, and in the boron zones are evident.

In replacing the vanadium alloy with other alloys, the neutron spectra have changed considerably, especially in the FW/breeder/reflector zones. An example of this change is shown in fig. 2, where the neutron fluxes in the outboard FW for the different alloys are shown relative to the neutron flux of the vanadium FW. The low energy neutrons (E < .1 eV) are two orders of magnitude higher in the iron-based alloys than in the vanadium alloy. This is due to the larger thermal absorbtion cross section of V and the larger elastic and inelastic cross sections of Fe for higher energy neutrons. In the magnet, the neutron flux using the vanadium alloy is about 10-12% higher, in all groups, than the neutron fluxes using the other alloys. This comparison shows that vanadium is less effective in attenuating the neutron flux than the other iron-based alloys. It also points to the necessity of consistent transport and activation calculations. Had any of the iron-based alloys' neutron flux been used in the vanadium alloy activation calculations, the results would be erroneous.

Using the vanadium alloys results in the highest tritium breeding ratio (TBR). The TBR of the vanadium case is 1.274 compared to 1.18 for the PCA and the tenelon alloys, and 1.198 for the HT9m alloy. The energy multiplication factor in the vanadium case is 1.22, and is very close to the energy multiplication factors in the HT9M and PCA cases. The energy multiplication factor of the tenelon alloy case is the largest and equals to 1.26.

Radioactivity

The radioactivity code RACC [5], has been used to calculate the radioactivity, the after-

heat, and the biological hazard potential for the TPSS design with the different structural materials after one year of continuous operation. For this time of operation, the average outboard and inboard fluence are 5.35 and 3.75 MWa/m^2, respectively.

Fig. 3 shows the radioactivity, per 1 cm height, of the outboard and the inboard FWs with the V15Cr5Ti alloy (right scale), and also shows the radioactivities of the iron-based alloys FWs relative to that of the vanadium alloy FWs (left scale). It is clear that the vanadium FWs have the least radioactivities all the time, except after about 1000 years where the low activation ferritic alloy HT9m FWs have the minimum radioactivities. At about 10 years from shutdown, the vanadium FWs radioactivities are 3 orders of magnitude less than the radioactivities of the iron-based FWs. This large difference is due mostly to the isotope ^{55}Fe. If fusion materials recycling is possible, this difference suggests that the vanadium alloys are more likely to be recycled, after a reasonable cooling period, than the iron-based alloys.

If we compare the radioactivities of the FWs, the breeder, and the reflectors (FW/B/R) for the different alloys, we find the same difference as in fig. 3 at about 10 years after shutdown. However, the magnitude of the difference is less than in the case of only the FWs in the period of about 1 year after shutdown. Also, the tenelon alloy joins the HT9m alloy in having less radioactivity than the vanadium alloy after 1000 years from shutdown.

As mentioned earlier, the vanadium alloy is less effective in attenuating neutrons than the iron-based alloys. This means that more neutrons will either interact with the other materials in the FW/B/R, e.g. with lithium producing more tritium, or they will find their way to interact with the shield producing more activation that would partly compensate for the large difference seen in fig. 3. Thus, if we compare the radioactivities of the whole TPSS design using the different alloys, fig. 4, we find, still, the vanadium alloy case has the minimum radioactivity for about 100 years, after which, the HT9m and the tenelon cases have the least radioactivities. The large difference between the vanadium case and

the other cases, due to ^{55}Fe at about 10 years from shutdown, has decreased from 3 orders of magnitude, in comparing only the FWs (fig. 3), to about two orders of magnitude in comparing the entire design.

The inboard W-reflector generates large part of the TPSS total radioactivity for about 1 year after shutdown. It produces 50 to 90% of the radioactivity in the vanadium alloy case and 35 to 60% of the radioactivity of the iron-based alloys cases. the isotopes ^{185}W, ^{187}W, and ^{181}W produced in the tungsten, which constitutes 80% of this zone, are the major contributing isotopes to the radioactivity in this zone, and consequently, to the radioactivity of the whole design.

After about two years from shutdown, the outboard and the inboard steel shields dominate the radioactivity in the vanadium TPSS design case and for about 500 years. Afterwards, the radioactivity though very small, is mostly due to the outboard CaO-reflector zone, where the long lived ^{14}C isotope had been produced by the $^{17}O(n,\gamma)$ reaction. In the PCA case, the outboard breeder zone dominates the radioactivity all the time after shutdown with large contributions from the FWs and CaO reflector. In the HT9m and the tenelon cases, the inboard and outboard breeder and FW zones have most of the radioactivity after one year from shutdown and for about 20 years. After that, the outboard/inboard steel shields generate most of the radioactivities until about 500 years from shutdown when the CaO zone becomes the major contributing zone to the TPSS radioactivity.

Fig. 5 shows the isotopic contributions to the V15Cr5Ti outboard FW radioactivity. Only isotopes contributing more than 2% of the radioactivity at any time are shown in this figure. The short-term activation in this alloy is due to the isotopes ^{52}V (3.75 m,$\bar{\gamma}$=1.45 MeV,$\bar{\beta}$=1.07 MeV), ^{51}Ti (5.76 m,$\bar{\gamma}$=.37 MeV,$\bar{\beta}$=.87 MeV), ^{51}Cr (27.7 d, $\bar{\gamma}$=.03 MeV, $\bar{\beta}$=.003 MeV), and ^{48}Sc (1.82 d, $\bar{\gamma}$=3.35 MeV, $\bar{\beta}$=.22 MeV). The longer-term activation is primarily due to ^{49}V (330 d, $\bar{\gamma}$=.9 KeV, $\bar{\beta}$=3.6 KeV). The long-term activation in this alloy is attributed to the transmutations of its impurities, N, O, Ni, Mo, and Nb.

The afterheat

One of the desirable characteristics of a fusion material is to have the minimum possible decay heat after being irradiated in the reactor. This decay heat depends on the the amount of the radioactive isotopes produced in the material and their disintegration energies that are associated with the emitted radiations, mostly γ and β radiations, from these isotopes. Large amount of afterheat would require a costly reliable active safety measurement to account for the possibility of a loss of coolant accident (LOCA) in the reactor[6,7].

Fig. 6 compares the integrated decay heats (IDHs) of the FW/B/R for the different alloys. Only in the first few minutes after shutdown, the HT9m and the PCA IDHs are slightly less than the V15Cr5Ti IDH. Afterwards, the vanadium alloy has the least IDH all the time. Accordingly, the use of the vanadium alloy in the TPSS design makes this design less vulnerable to a LOCA than in the case if any of the other alloys, specially the tenelon alloy, had been used. However, the tungsten reflector dominates the afterheat of the whole design for about 1 y after few minutes from the shutdown. Fig. 7 shows the isotopic contributions to the afterheat of the vanadium outboard FW. Here, the isotopes are weighted not only by their concentrations, but also by their decay energies. It is worth noting that large part of this alloy afterheat is generated by the transmutations of its Ti content.

The biological hazard potential

The air-biological hazard potential of a material gives a measurement of the impact of such material on the environment in case of a catastrophic accident. In comparing the BHP-air of the different cases, the vanadium alloy case has the least BHP-air. The BHP-air of the entire design and for all the alloys is attributed mostly to the W reflector. With respect to the BHP-air of the vanadium alloy, isotopes generated by the Ti transmutations dominate the BHP-air of this alloy.

Conclusions

It is important in guiding the process of fusion materials selection to have a coherent transport and activation analyses for the materials in the context of an entire design of a fusion reactor. Zero dimensional analyses using a fixed known neutron spectrum will always lead to distorted conclusions overlooking the effects of the materials on the neutron spectrum and the importance of other parts of the design to the activation issues of fusion reactors. As seen in these analyses, The vanadium alloy, the V15Cr5Ti, has the least radioactivity, afterheat, and BHP-air compared to other leading fusion structural steels. As a result, this alloy has the largest possibility of recycling, the least vulnerability to a LOCA, and the minimum impact on the environment. However, the results also indicate that the use of other materials in the system can have a substantial impact on the overall activation issues. For example, the use of tungsten for enhanced shielding contributes significantly to the short-term activation in the TPSS design.

References

[1] D.L. Smith et al., Argonne National Laboratory, ANL/FPP-84-1 (1984).

[2] D. Ehst et al., Argonne National Laboratory, ANL/FPP/86-1 (1987).

[3] H. Attaya and M. Sawan, Fusion Technology 8/1(1985)608.

[4] R. O'Dell et al., Los Alamos National Laboratory Report, LA-9184-N (1982).

[5] J. Jung, Argonne National Laboratory, ANL/FPP/TM-122 (1979).

[6] H. Attaya et al., Fusion Technology, 15(1989)893.

[7] H. Attaya, Fusion Technology, 19(1991)1331.

Figures

Fig. 1. The TPSS radial build and the neutron flux for the vanadium case.

Fig. 2. The neutron fluxes in the outboard FW. Right axis: the vanadium case, left axis: the iron-based alloys' cases relative to the vanadium case.

Fig. 3. The outboard FW radioactivities for the iron-based alloys (left axis) relative to the vanadium outboard FW radioactivity (right axis).

Fig. 4. The radioactivities of the whole TPSS design for the iron-based alloys (left axis) relative to the vanadium case (right axis).

Fig. 5. The isotopic contributions to the vanadium outboard FW radioactivity.

Fig. 6. The integrated decay heats in the FW/B/R zones for the iron-based alloys (left axis) relative to the vanadium case (right axis).

Fig. 7. The isotopic contributions to the vanadium outboard FW afterheat.

Table 1. Alloys' Compositions

Alloy:	V15Cr5Ti	PCA	HT9m	Tenelon
$\rho(gm/cc)$:	6.1	8.0	7.8	8.0
B	-	0.005	0.001	0.001
C	0.005	0.005	0.15	0.15
N	0.01	0.01	0.001	0.005
O	0.01	-	0.007	0.007
Al	0.02	0.03	0.008	0.008
Si	0.03	0.5	0.2	0.2
P	0.003	0.01	0.013	0.013
S	0.001	0.005	0.004	0.004
Cl	0.0001	-	-	-
K	0.00001	0.0003	0.0003	0.0003
Ti	5.	0.3	0.1	0.003
V	79.91349	0.1	0.3	0.002
Cr	15.	14.	11.	15.
Mn	-	2.	0.53	15.
Fe	0.004	64.8584	85.16493	69.57593
Co	-	0.03	0.005	0.005
Ni	0.0004	16.	0.006	0.006
Cu	0.0002	0.02	0.003	0.003
As	0.0002	0.02	-	-
Zr	-	0.005	0.001	0.001
Nb	0.0004	0.03	0.00011	0.00011
Mo	0.001	2.	0.00027	0.00027
Ag	-	0.0001	0.00009	0.00009
Cd	-	0.0002	0.0001	0.0001
Sn	-	0.005	0.003	0.003
Sb	-	0.001	0.0005	0.0005
Ba	-	0.001	0.0002	0.0002
Tb	-	0.001	0.0002	0.0002
Ta	0.001	0.01	0.0004	0.0004
W	0.0002	0.05	2.5	0.01
Ir	-	0.001	0.0002	0.0002
Pb	-	0.001	0.0005	0.0005
Bi	-	0.001	0.0002	0.0002

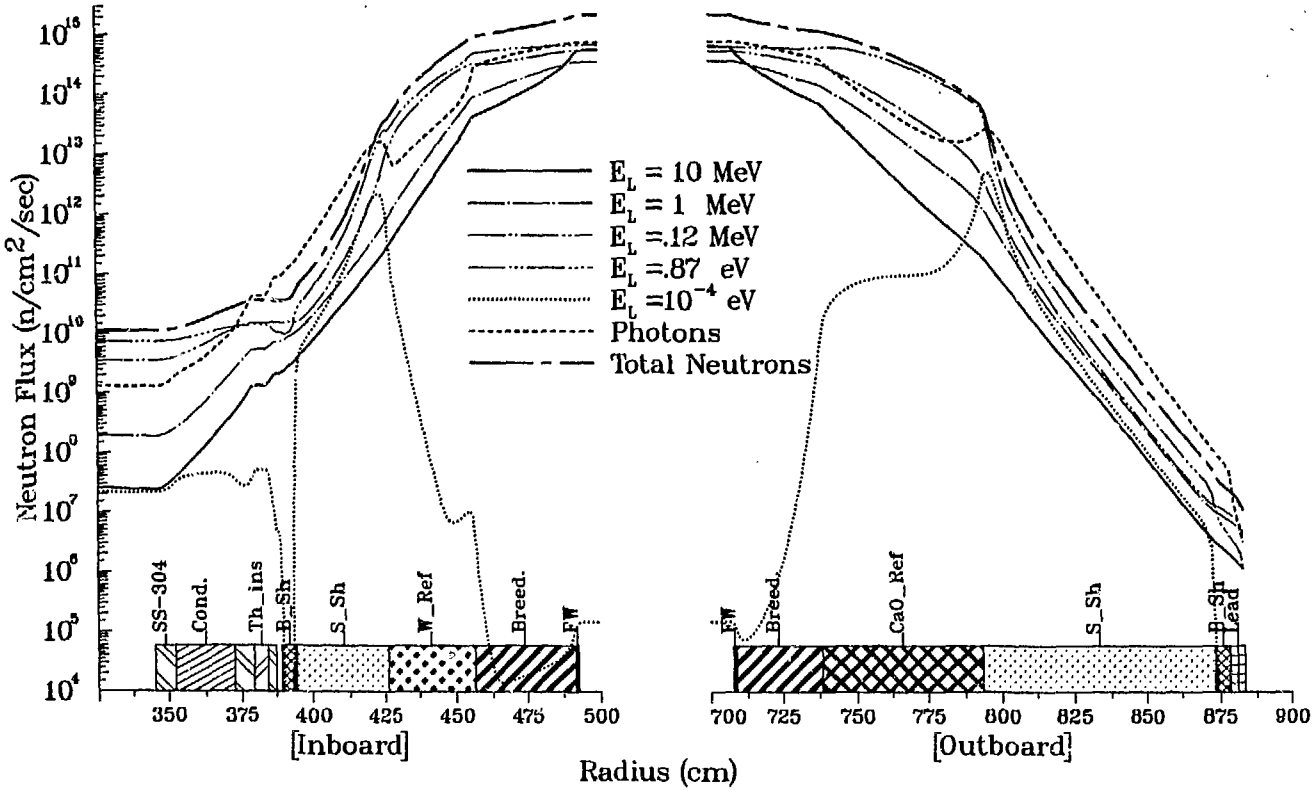
Neutron Flux (n/cm^2/sec)
10^{15}
10^{14}
10^{13}
10^{12}
10^{11}
10^{10}
10^{9}
10^{8}
10^{7}
10^{6}
10^{5}
10^{4}
E_L = 10 MeV
E_L = 1 MeV
E_L = .12 MeV
E_L = .87 eV
E_L = 10^{-4} eV
Photons
Total Neutrons
SS-304
Cond.
Th_ins
B_Sh
S_Sh
W_Ref
Breed.
FW
350
375
400
425
450
475
500
[Inboard]
FW
Breed.
CaO_Ref
S_Sh
B_Sh
Lead
700
725
750
775
800
825
850
875
900
[Outboard]
Radius (cm)

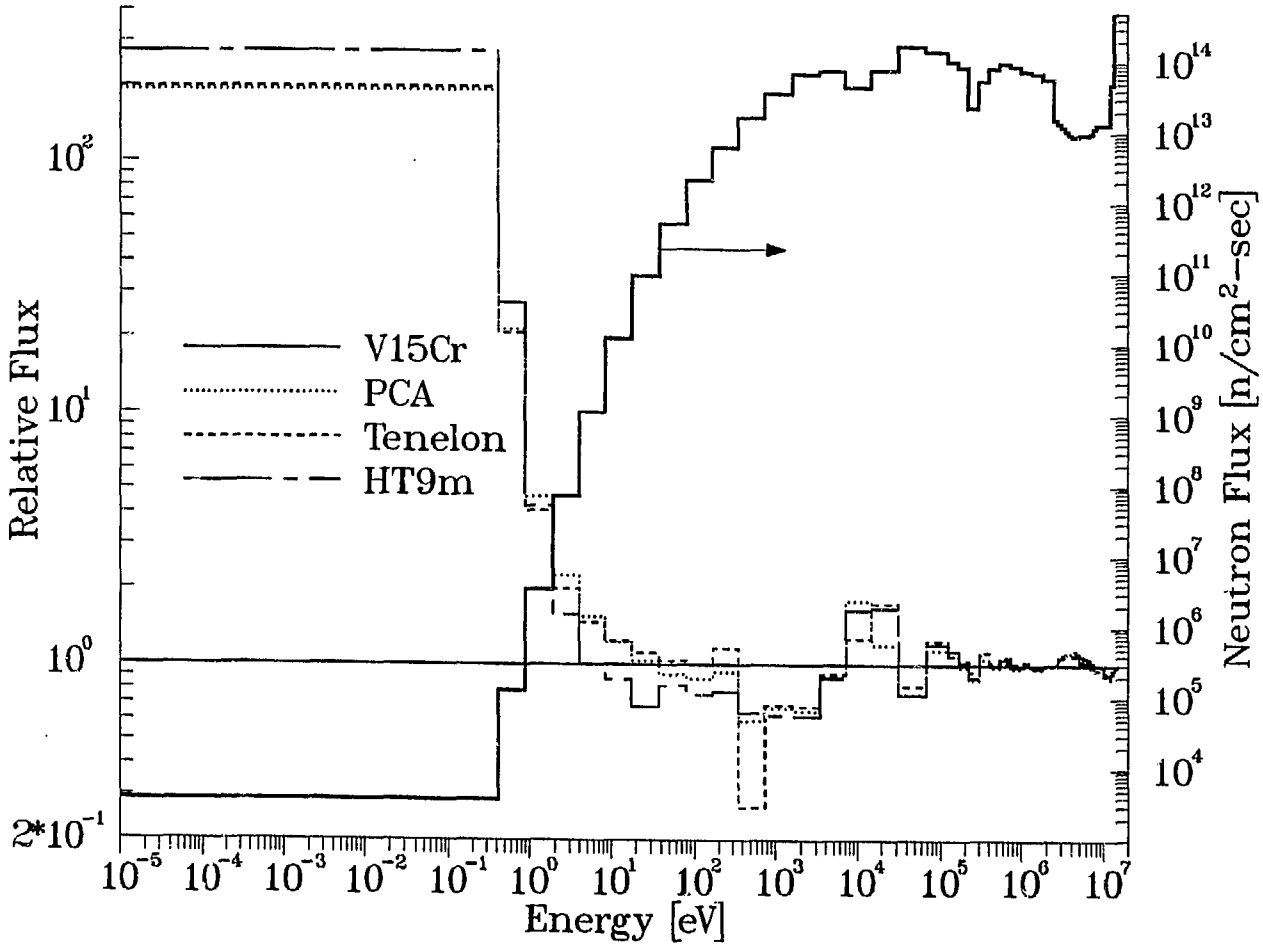
Relative Flux
Neutron Flux [n/cm²-sec]
Energy [eV]
V15Cr
PCA
Tenelon
HT9m
2*10⁻¹
10⁰
10¹
10²
10⁴
10⁵
10⁶
10⁷
10⁸
10⁹
10¹⁰
10¹¹
10¹²
10¹³
10¹⁴
10⁻⁵
10⁻⁴
10⁻³
10⁻²
10⁻¹
10⁰
10¹
10²
10³
10⁴
10⁵
10⁶
10⁷

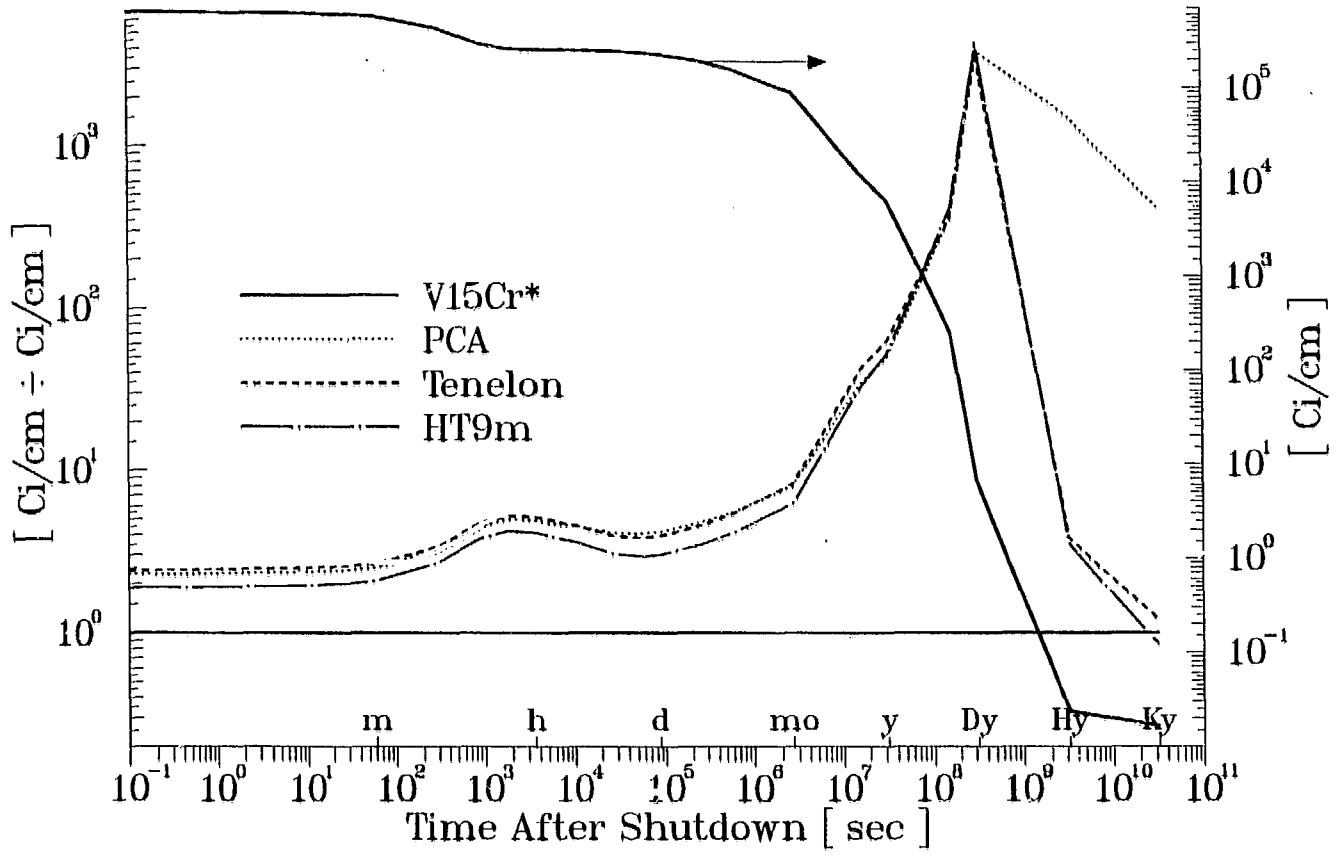
[Ci/cm ÷ Ci/cm]
[Ci/cm]
V15Cr*
PCA
Tenelon
HT9m
m
h
d
mo
y
Dy
Hy
Ky
Time After Shutdown [sec]

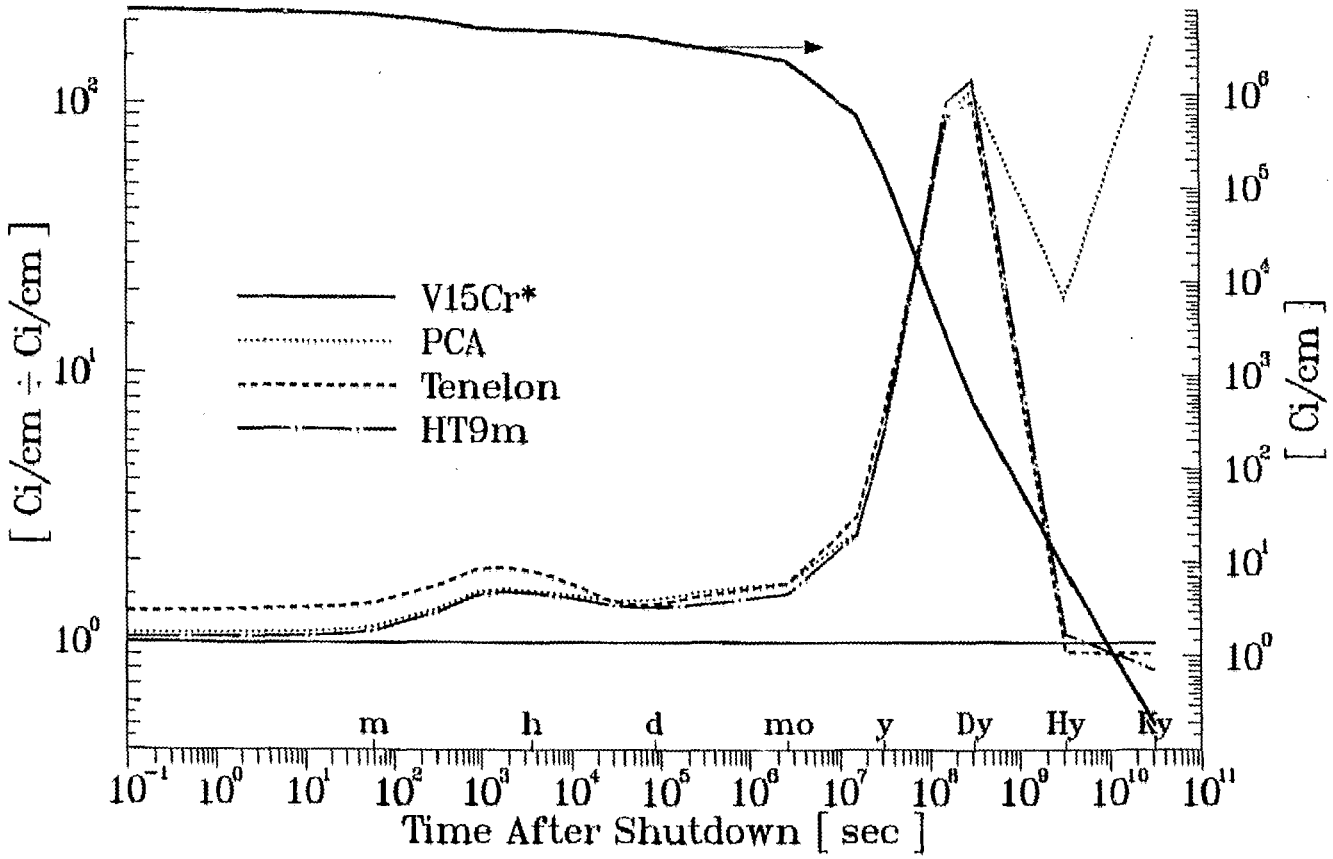
[Ci/cm ÷ Ci/cm]
[Ci/cm]
V15Cr*
PCA
Tenelon
HT9m
m
h
d
mo
y
Dy
Hy
Ky
Time After Shutdown [sec]

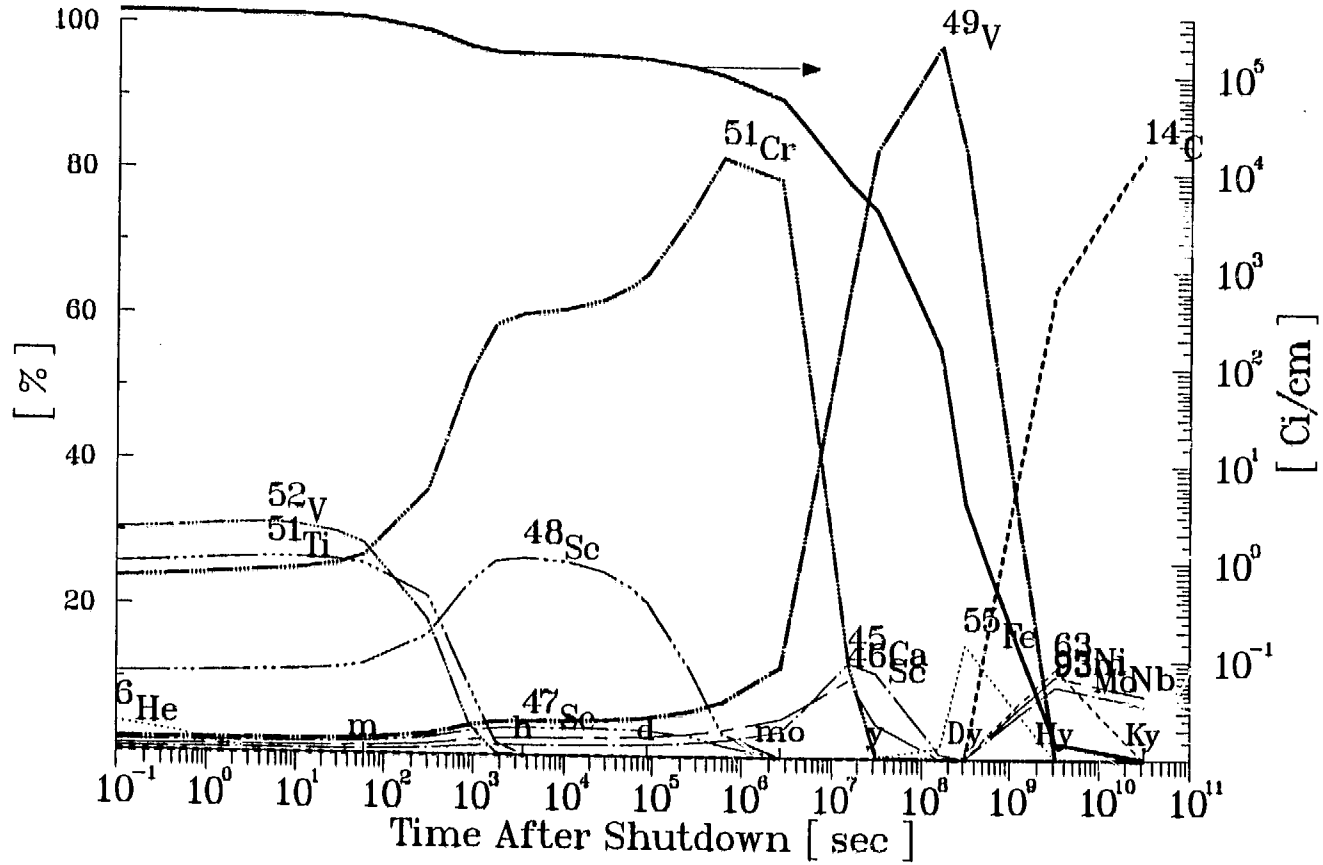
100
80
60
40
20
[%]
49V
51Cr
14C
52V
51Ti
48Sc
6He
47Sc
45Ca
46Sc
55Fe
63Ni
93Mo
93Nb
m
h
d
mo
y
Dy
Hy
Ky
10^{5}
10^{4}
10^{3}
10^{2}
10^{1}
10^{0}
10^{-1}
[Ci/cm]
10^{-1} 10^{0} 10^{1} 10^{2} 10^{3} 10^{4} 10^{5} 10^{6} 10^{7} 10^{8} 10^{9} 10^{10} 10^{11}
Time After Shutdown [sec]

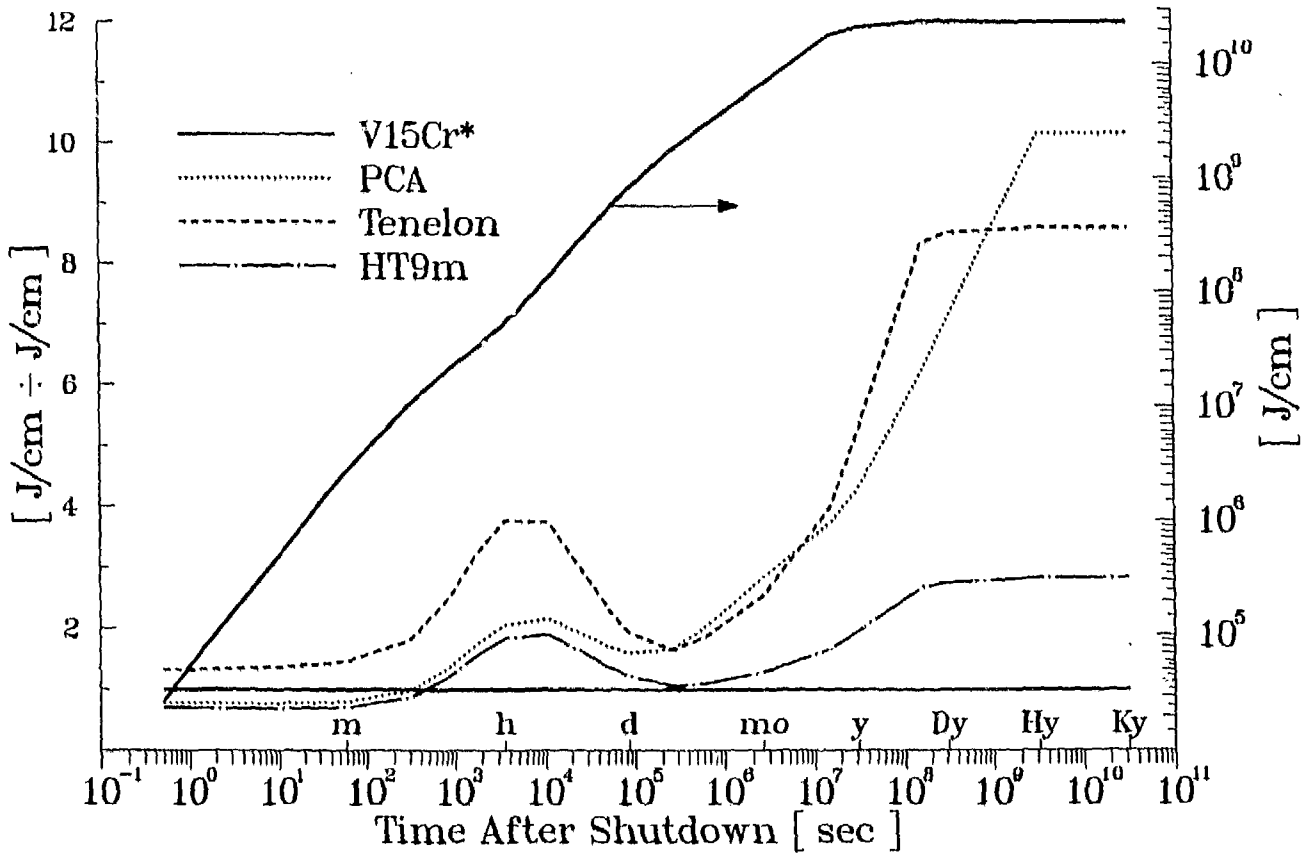
V15Cr*
PCA
Tenelon
HT9m
[J/cm ÷ J/cm]
[J/cm]
12
10
8
6
4
2
10^{10}
10^{9}
10^{8}
10^{7}
10^{6}
10^{5}
m
h
d
mo
y
Dy
Hy
Ky
10^{-1} 10^{0} 10^{1} 10^{2} 10^{3} 10^{4} 10^{5} 10^{6} 10^{7} 10^{8} 10^{9} 10^{10} 10^{11}
Time After Shutdown [sec]

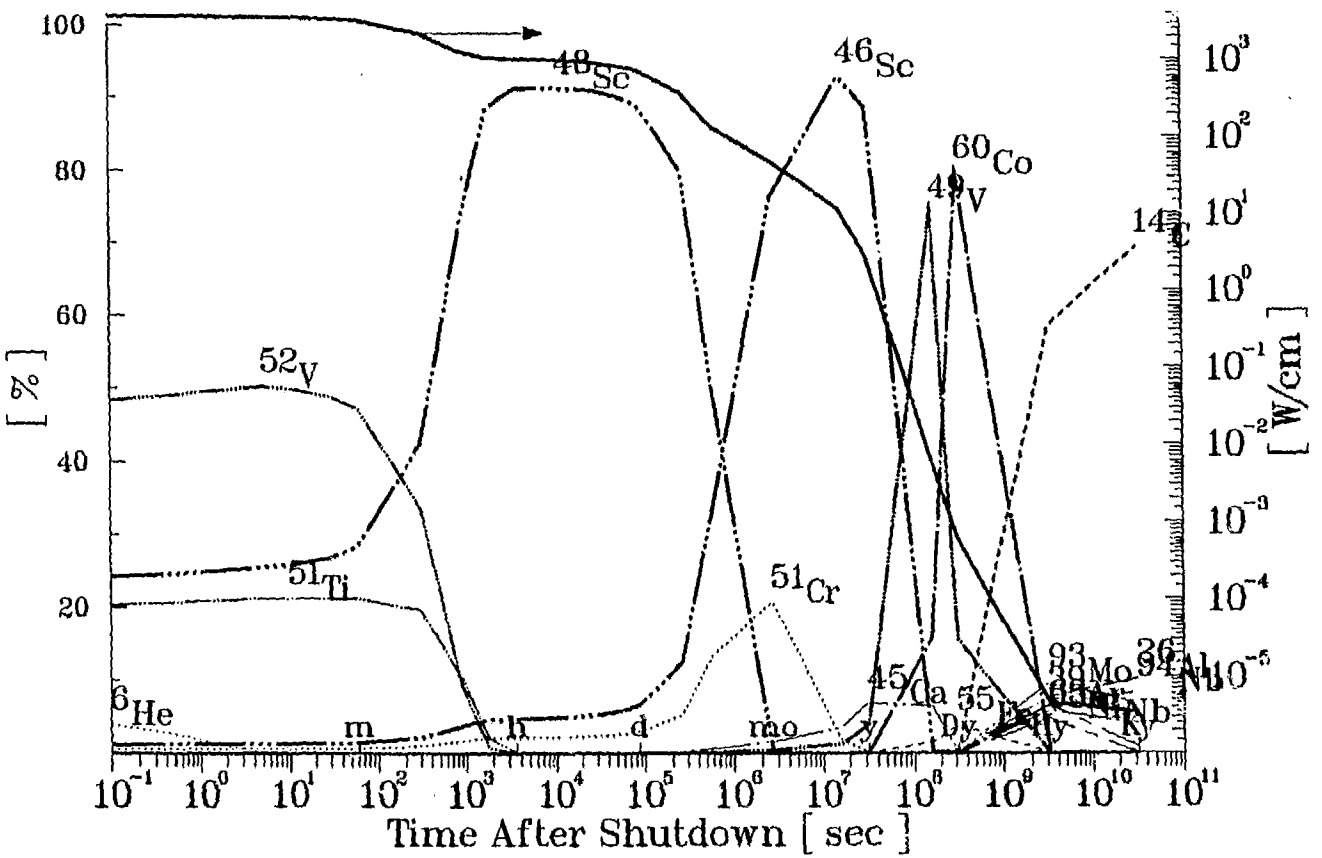
100
80
60
40
20
[%]
10^{3}
10^{2}
10^{1}
10^{0}
10^{-1}
10^{-2}
10^{-3}
10^{-4}
10^{-5}
[W/cm]
^{48}Sc
^{46}Sc
^{60}Co
^{49}V
^{14}C
^{52}V
^{51}Ti
^{51}Cr
^{6}He
^{45}Ca
^{55}Fe
^{93}Mo
^{36}Cl
^{94}Nb
m
h
d
mo
y
Dy
Ty
Ny
10^{-1} 10^{0} 10^{1} 10^{2} 10^{3} 10^{4} 10^{5} 10^{6} 10^{7} 10^{8} 10^{9} 10^{10} 10^{11}
Time After Shutdown [sec]